SSC22-WKVI-03

Utilizing Additive Manufacturing of Semi-Crystalline Thermoplastics and Topology Optimized Generative Designs for Complex Small Satellite Bus Geometries

William Hunter Bradford, Aidan Delliponti, Ryan Formel
University of Georgia Small Satellite Research Laboratory
1510 Cedar St, Athens, GA, 30602
970-682-3398, whbradford.99@gmail.com

ABSTRACT

Small satellite buses have traditionally been manufactured through subtractive means and ultimately limiting capability in feature, form, and an inability to alter the volumetric density of the material. However, emergent additive manufacturing methods that utilize Fused Deposition Modeling (FDM) integrated with soluble support material allow us to print synthetic thermoplastics, such as Polyetheretherketone (PEEK). Consequently, the number of structural parts and hardware components is reduced, along with the cost. Structural strength and dimensional stability of PEEK are comparable to traditional aluminum alloys in the construction of most satellite components. Additive manufacturing further allows the implementation of topology optimization algorithms to develop and produce complex geometries with resolutions up to 5μm in x/y movements and 1μm in z movements. Thermoplastics possess ideal strength to weight ratios and thermal expansion coefficients that can be exploited to design more desirable components of small satellite buses. We believe that topology-optimized, 3D-printed small satellite frames made from PEEK can offer a lighter alternative to their metal alloy counterparts. To show this, we will demonstrate the generative optimization of the SPectral Ocean Color (SPOC) satellite's 3U frame and compare its structural, thermal, and modal analysis simulations to those of an optimized design.

INTRODUCTION

In recent times, the space industry has radically changed as academic and commercial entities have begun investing vast amounts of time and funding toward private satellite missions. Through the regulation of small satellite sizes and weights, CubeSat programs have revolutionized accessibility to Low Earth Orbit (LEO) by standardizing physical mission constraints, deployment mechanisms, and rideshare programs. Additionally, due to a CubeSat's low cost, it is a remarkably low-risk option to consider when attempting to test modern technologies in space applications without jeopardizing high-risk missions during the exploratory testing phase. Such technologies include topology optimization algorithms, additive manufacturing techniques, and the inclusion of thermoplastics in structural components.

Topology optimization (TO) is a numerical method that optimizes the distribution of the material in a structural component based on a constraint, whether that is accelerated loading, mechanical vibrations, or difference in thermal distributions. The implementation of TO in model-based design is not a new concept, but it has proven rather difficult to apply to tangible parts due to limitations imposed by subtractive manufacturing.

However, the emergence of additive manufacturing techniques has begun to prove TO applications in industries such as automotive, medical devices, robotics, and many more. 3D printing is among the forerunners of additive manufacturing techniques due to its wide availability, low cost, and ability to use a multitude of different materials with varying mechanical properties. 3D printers have the ability to print at extremely high temperatures with high tolerances at a relatively rapid pace, allowing a user to prototype and manufacture quite literally anything they can imagine.

One example of a notable material relevant to the space industry that is enabled by 3D-printing technologies is polyetheretherketone (PEEK). This type of thermoplastic from the polyaryletherketone (PAEK) family is a semi-crystalline polymer that exhibits exceptional mechanical properties, high-temperature resistance, and very low outgassing tendencies. PAEK's exceptional material performance is related to the rigid nature of the repeating unit Figure 1, which consists of aromatic molecules linked by in-chain ether and ketone functional groups [12].

The above technologies can tremendously impact the way in which small satellite buses are designed and manufactured by redistributing indispensable weight to the scientific payload. Furthermore, they can be scaled far beyond the applications of small satellites to include smaller structural components on rockets, satellites, space stations, etc. The benefits are interminable which

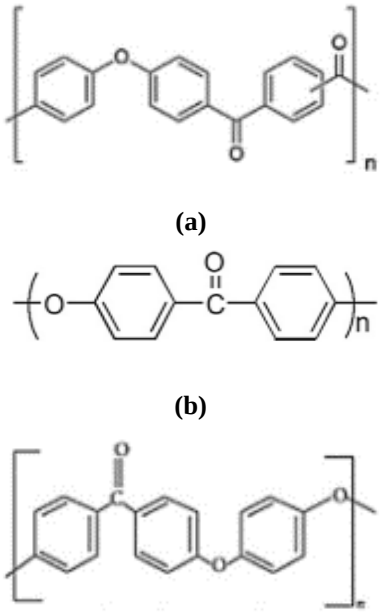

(a)

(b)

(c)

Figure 1: Repeating unit of (a) PEKK, (b) PAEK, and (c) PEEK

raises the question: why are topology optimization, additive manufacturing, and space-grade thermoplastics not utilized in the space industry?

The goal of this research is to prove that the combination of these modern technologies is a suitable mechanical solution for cost-efficient, reproducible, and structurally sound small satellite buses in the future. This paper serves as a case study comparing the University of Georgia's (UGA) original SPectral Ocean Color (SPOC) 3U cubesat frame to one recently redesigned out of PEEK that underwent structural, modal, and thermal finite-element simulations to validate topology optimization algorithms on PEEK satellite frames.

MATERIALS AND METHODS

Design Criteria

The technical requirements for SPectral Ocean Color (SPOC) mission were to operate in low Earth Orbit (LEO) at an altitude of 405km as well as abide by the requirements set forth by the Antares User's Guide for launch. Once in orbit, the rocket was launched to the International Space Station for handoff and satellite deployment. The mechanical requirements provided in [17], are provided in Table 1.

Model-Based Design and Implementation

The initial procedure used for running the simulations

Simulation Requirement	Units	Axis	
		Axial	Lateral
Structural	Acceleration (G)	-1/+6.5	±1.5
Modal	Frequency (Hz)	5-100	5-100

Table 1: Mechanical Requirements per Antares User Launch Guide

through Ansys Workbench R1 consisted of a modification to both the payload and frame of the original SPOC model-based designs. These modifications, outlined in Figure 2, show the adjustments made to the assembly using CAD software. The figures on the left illustrate the original payload, and the figures on the right are a simplified version of the former. These simplifications are a practical approach to ensure ease of use and proper work solutions when processing the assembly through Ansys software packages. Utilizing a simplified payload also leads to better results when modeling a topology optimized frame as node clusters cause significant

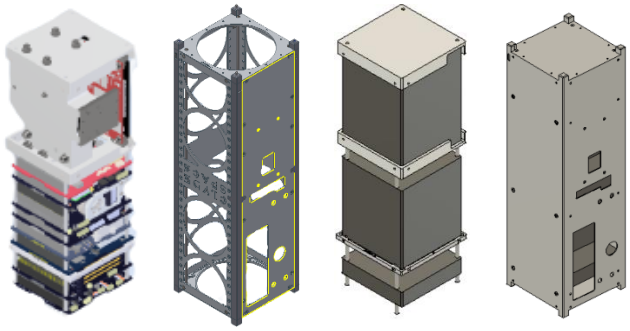

Figure 2: Original (2x left) and Modified (2x right) Models

interference in the simulation software as well as unnecessary complications. Further care was taken to avoid tight clusters of nodes during the meshing operation by removing all radii and unnecessary holes from the assemblies.

The electronics stack consists of the components listed in Table 2. All boards have a standard perimeter measuring 90 mm x 96 mm (PCI104 Standard). Dimensions in the z-direction are not included due to not being necessary in the simplified stack model. All other included measurements were appropriately captured while making the simplified model, including the overall weight and center of mass, which was overwritten by the user.

The electronics stack was further simplified to be modified as a single material representative of the whole stack, whose physical properties are provided in Table 3.

Component	Mass (g)	Max Instantaneous Power Draw (W)
PYLD	106.9	1.986
CDH	205.4	4.246
EPS	901	1.444
COMM	352.7	5.836
ADCS	335	0.453

Table 2: Payload components with mass and max power draw

Property	Frequency
Density	1.957 g/cm^3
Linear Isotropic Elasticity	205 MPa
Mass	1.901 kg
Volume	0.001139 m^3
Youngs Modulus	190 GPa
Thermal Conductivity (max)	14 W/m·K
Thermal Expansion (max)	18·10e-6 1/K
Specific Heat (max)	530 J/kg·K
Poisson's Ratio (min)	0.265

Table 3: Simplified Properties of Electronics Stack

Modal Simulation Implementation

Ansys was used to conduct the modal analysis of the system as well as provide the TO design from the results. The solution obtained for the natural frequencies of the assembly is then processed through Ansys's topology optimization program, where mass is kept in the necessary regions of the frame that correspond to a range of predetermined frequencies experienced during flight.

The frame was assumed to be launched in the upright position, so it was fixed on both its Z+ and Z- faces during the simulation as these were the faces supported by the deployer. A random vibration test was used in order to identify the first 6 lowest modes of the satellite bus and a mechanical deformation analysis was performed to find the maximum deflection during resonance.

The modal and structural analysis in Ansys does not support the ability to test materials with anisotropic mechanical properties, so for the purposes of the model, the mechanical properties corresponding to a raster angle of H-90° were used. This is less than the material's maximum mechanical properties and when applied to the mesh it can be assumed that the frame will be well within tolerance when running the simulations. This raster angle and its associated properties are a reasonable means of fabricating such a frame with minimal distortions during the manufacturing process.

Structural Simulation Implementation

This simulation was performed in order to determine whether a PEEK frame would reach fracture under either axial or lateral loading during launch. The analysis included conducting the equivalent elastic strain, total deformation, and directional deformation of the system. SPOC's orientation was again assumed to be aligned with the resultant forces parallel to the z-axis of the satellite. Since CubeSats <5kg have issues with obtaining an accurate envelope for expected loads so a respective factor of safety of N=2.0 was used within the simulation [16].

Fixturing was again applied on both the Z+ and Z- faces while conducting the simulations. The inertial loading analysis determines total deformation and equivalent stress under launch conditions. The acceleration used in the simulation was determined using the JPL Mass-Acceleration Curve, with the projected mass of SPOC at 3.64 kg. The resultant acceleration is approximately 42 G's (gravitational acceleration), or 412.02 m·s^{-2}. Accelerations of 42 G's were applied to the frame in both the axial and lateral cases.

Steady-State Thermal Simulation Implementation

Workbench was once again used to implement steady-state thermal simulations that were modeled to be representative of the satellite in orbit. In order to effectively simulate the space environment, there are several heat sources that must be included in the analysis. The thermal loads were categorized as follows:

- Internal Heat Load: Internal heat is generated from the electronics stack while operating in orbit. All devices within the payload stack were assumed to be operating in "image mode" as this mode is tested to produce the max instantaneous internal heat of 13.965 watts, as noted in Table 3. This data was collected at one-minute increments during a power budget test lasting six hours. The tabulated data was directly imported to Ansys.
- External Heat Load: Satellites experience many external heat loads during orbit including solar heat fluxes, primarily direct sunlight and reflected albedo. Additionally, the Earth also emits infrared energy. These sources are simplified in Table 4. The external faces of the frame itself will be covered by solar panels on all faces except for the X+ and Z- faces, but an emissivity and absorptivity, representative of

the solar panels, of 0.45 were selected for all faces to simplify the simulation.

The thermal loads are summarized in Table 4.

Heat Source	Flux ($W \cdot m \cdot s^{-2}$)
Direct Sunlight	290
Albedo	70
IR Energy	70
Beta Angle Correction	.04 (unitless)
Internal Heat Generation	13.965

Table 4: External, Internal Heat Loads and Correction Factor

SPOC's orbit was in LEO at an elevation of 400 km with an average beta angle of 70°. The data in the table above accounts for each of these variables and are the average over an entire orbital period, including when the satellite is both in direct view and hidden from the sun. Thus, these values were input as constants over the duration of the simulation. Due to average values being used, the final thermal gradient will not be representative of the max hot or cold case of the satellite, but rather a general idea of the heat trends.

The result of the thermal simulation provides a temperature gradient that displays both the location and thermal load across the entirety of the frame. In order to optimize this, we removed portions of the frame that received significantly less thermal load than the surrounding area. This ensured that thermal integrity remained paramount while still drastically reducing overall weight.

Mechanical Properties of FDM Printed PEEK

Prior research has demonstrated a comparative analysis on the additive manufacturing processing conditions needed to obtain optimal mechanical properties for FDM 3D-printed PEEK. Such parameters include high printing temperature and bed temperature, and printing orientation. The reported parameters in the literature for FDM 3D-printed PEEK are listed in Table 5.

Such parameters were used when examining specimen materials in flexural and tensile testing at different raster angles. These raster angles are crucial in understanding the physical limitations of 3D printed PEEK as the

Parameter	Value
Raster angle	0 [3]
Layer Thickness	0.1-0.3 mm [5]
Ambient temperature	150-200 C [6]
Nozzle Temperature	420-440 C [7]
Print speed	20 mm/s [8]
Infill	100%
Heat treatment method	Annealing [6]

Table 5: Ideal FDM Print Settings for PEEK

structure itself cannot be treated with the same properties as injected molded samples. This is because FDM materials possess an anisotropic property that is pronounced due to the limitations of layer adhesion, non-uniform cooling, layer heights, and chamber temperatures. For PEEK, layer cooling is crucial for ensuring proper capitalization of the material properties.

The differences in material properties from injected molded PEEK [3] are due to the formation of voids at cross junctions between beads as well as inconsistent crystallization rates. These inconsistencies can become more apparent when fabricating larger structures as it is challenging to achieve consistent rates of cooling within the build chamber [13]. Proper post-processing of the print aids has been suggested to improve mechanical performance in certain settings, but the data is inconclusive in determining if the practice has a significant impact. However, other printer settings appear to contribute to the bulk of improved mechanical properties. Removing porosity improves overall mechanical properties, however, the percent of crystallization is unlikely to exceed 45-50%. With some samples retaining a maximum of 96% of bulk materials strength with proper fabrication settings [18].

The filament used to produce specimens for testing in the literature [3] was 1.75 mm diameter Victrex® PEEK 450P [14]. The filament exhibits glass transition and melting temperatures of 153 °C and 340 °C respectively, as found in the Victrex® PEEK 450P database.

As seen in Figure 3, the difference in raster angle dramatically changes the mechanical properties. Where molded PEEK samples retain the maximum mechanical properties in Table 6, the lowest of values structurally appear at a raster angle of V-90°. This is exceptionally true for tensile-tested values, but for the purposes of the SPOC mission, exceptional tensile elongation and strength are not required.

	Raster Angle	H-0	H-90	V-90	PEEK 450G
Tensile Props.	Young's Modulus (GPa)	3.8 ± 0.03	3.54 + 0.05	3.03 + 0.01	4.0
	Tensile Strength (MPa)	82.58 + 1.03	72.88 + 1.92	9.99 + 0.94	98
	Tensile Elongation	110.97 + 5.31	2.91 + 0.14	.33 + 0.03	4.5
	Poisson's Ratio, v	0.44 + 0.02	0.43 + 0.01	0.37 + 0.005	1
Flexural Props.	Flexural Modulus (GPa)	3.08 + 0.22	3.06 +0.21	2.54 + 0.07	3.8
	Flexural Strength (MPa)	142.0 + 5.56	124.3 + 7.98	16.40 + 2.18	165

Table 6: Tensile vs. Flexural Properties of PEEK [3]

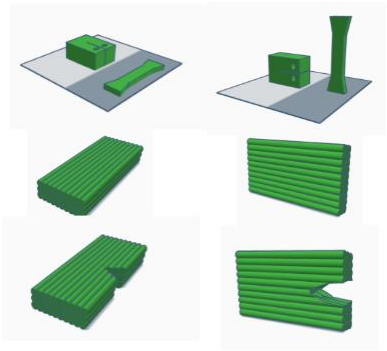

Figure 4: FDM of PEEK Samples in tensile and compression tests. Left shows 0º beads orientation; right shows 90º bead orientation.

PEEK Material Properties	Typical Value
Density	1.3 g/cm^3
Thermal Expansion Coefficient	140 ppm/k
Heat Deflection Temperature	152 C
Thermal Conductivity	0.32 W/ m·k
Elongation at break (%)	45
Compressive Modulus	3.2 GPa
Compressive Strength	125 MPa
Shore D Hardness	84.5
Water Absorption	0.45%
Ultimate Tensile Strength	78.0 ± 7.2 MPa
Max Stress	173 ± 8 MPa

Table 7: PEEK Material Properties [9]

Off-Gassing

In accordance with the ECSS-Q-ST-70-02C standards [10], materials qualified for space-based applications must meet the following criteria and procedures for proper adoption into a mission's payload: Recovered Mass Loss (RML) < 1.0% and Collected Volatile Condensable Material (CVCM) < 0.10%. The requirements of RML and CVCM may require even lower minimum values for materials used in the fabrication of optical devices, or in their vicinity. For the purposes and mission of SPOC the off-gassing values for PEEK printed frames are within the minimum tolerance limit after proper post-processing procedures. The values illustrated in Table 7 [11] and Table 8 [1] are measured at 0.11% and 0.01% for RML and CVCM respectfully.

Density Measurements	Density (g/cm^3) From Datasheet [15]	Density (g/cm^3) Measured [15]
PEEK 3D Tensile Sample	1.300	1.221 ± 0.036
PEEK 3D Outgassing sample	1.300	1.244 ± 0.025

Figure 8: Density at different RML and CVCM

To ensure such values are met it is practical to bake critical hardware to the highest permissible temperature for a prolonged time in order to remove residual contaminants. For the requirements of the SPOC mission using proper annealing procedures after printing will ensure tolerable off-gassing values [3].

RESULTS AND DISCUSSION

Modal Simulation Results

The modal analysis performed on the simplified frame and payload produced the following results outlined in Table 9, with the first and lowest mode being 249.3 hz. This provides a factor of safety just under 2.5 for the satellite when compared to the minimum lowest mode of 100hz required by the launch provider. However, since this simulation did not include fasteners, individual electronics boards or payloads, the actual modes will be lower than those received. However, they provide a good indication of whether the PEEK frame will be

structurally rigid enough to support the satellite during launch.

Additionally, the total deformation results of the mechanical analysis also stayed within acceptable tolerances, with a maximum deformation of 0.04514 mm. Hence, inspection of the results from both the modal analysis demonstrates that the PEEK frame is capable of meeting the vibrational requirements of the launch provider's specifications.

Mode	Frequency
1st	249.3 Hz
2nd	333.9 Hz
3rd	472.29 Hz
4th	481.92 Hz
5th	500.32 Hz
6th	521.76 Hz

Table 9: Modes of the PEEK frame

Structural Simulation Results

The structural simulations necessary to establish a TO frame include a total deformation, directional deformation, and equivalent elastic strain analysis outlined in the figures below. As seen, there is minimal deformation during loading as shown in Table 10. These results prove to be acceptable for the requirements set forth by Antares for the structural rigidity of the frame. There are no major concerns with the simulations, especially considering that no major deformation occurs that could affect either the stability of the electronics stack. In addition to the results of the modal simulations, these results show promise when considering PEEK as a major structural component for future satellite missions.

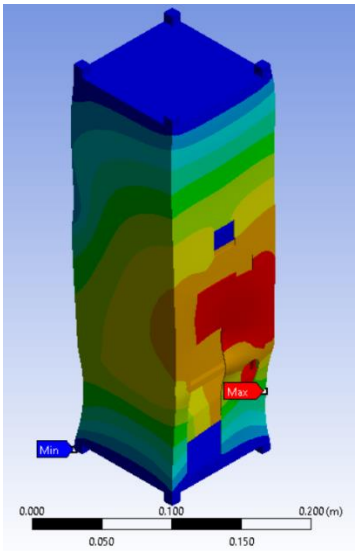

Figure 5: Results of Total Deformation Simulation

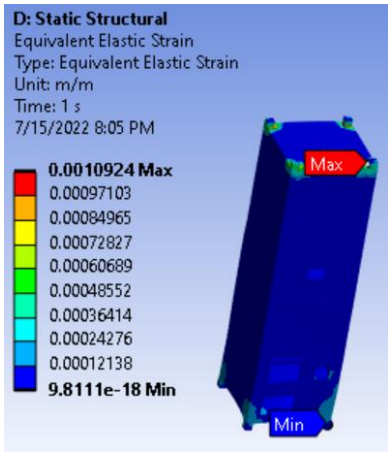

Figure 6: Results of Equivalent Elastic Strain Simulation

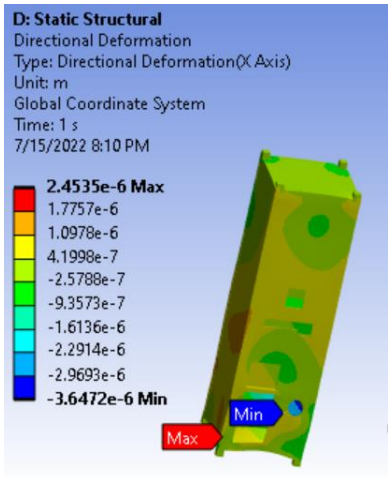

(a)

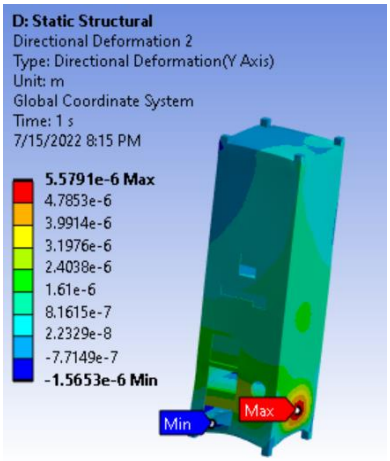

(b)

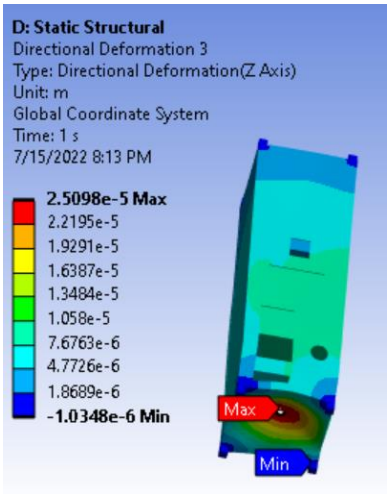

(c)

Figure 7: Results of Directional Deformation in (a) x-axis, (b) y-axis, and (c) z-axis

	Equiv. Elastic Strain	Total Deform.	Directional Deform.		
			x	y	z
Deform.	2.49e -5	6.49e-6	2.45 e-6	5.58 e-6	2.51 e-5

Table 10: Results of Directional Deformation Simulation

The Directional Deformation simulations are not accurate to the true nature of an anisotropic material such as FDM PEEK. However, they do show an approximation of the directional deformation for the assumed orientation experienced during launch as seen in Figure 6.

Thermal Simulation Results

The thermal simulation results proved inconclusive for this paper. They were riddled with problems during implementation even with the simplifications and assumptions made during the design process and we were unsuccessful in receiving an outcome we were confident enough to present in this paper. Other literature has explored similar space applications for PEEK and has proven desirable results are obtainable. However, these results proved better suited for smaller applications such as 1U models.

Topology Optimization Results

Using the results gathered from the Static Structural and Modal vibration simulations the topology optimization could be determined using the Ansys workflow. This model acts as a TO representation of the frame suited for the environment experienced at launch without the addition of the thermal steady-state heat flow results. This produced the image seen in Figure 7 which shows a majority of the material removed from the X+/- and Y+/- faces which ultimately leads to a significant decrease in weight compared to its Aluminum counterpart. The final PEEK TO frame had a proportional mass of 131.6g to the original mass of the 238.4g Aluminum frame.

These weight reductions not only correlate to more mass that could be placed elsewhere in more robust or powerful electronics but also to decreases in both the launch and manufacturing costs of the satellite as a whole. Launching is typically priced per kg, and while 131g may not be much compared to the total mass of the satellite, those savings alone total higher than $1000 USD per launch. 3D printing is also generally significantly cheaper than machining, requiring much fewer man hours and attention to detail, allowing the final customer to realize their physical design much sooner than was available before.

Although this frame may appear to be sporadic and non-uniform, the distribution of weight is such that the frame will still provide acceptable modal and structural strengths under loading conditions. It has more than enough surface area to stabilize the required electronic stack and mount the solar panels to each face while leaving proper routing for both harnesses and mechanical interfaces. Any critical areas not covered by solar panel assemblies can be shielded using foil or other

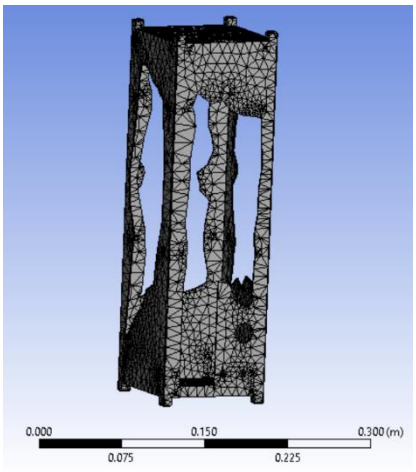

Figure 8: Final Topology Optimized Frame Design

reflective materials to limit radiation entering the center of the frame.

CONCLUSION

This study investigated the use of the semicrystalline polymer material PEEK manufactured using FDM methods for small satellite frame applications. The 3D model used for the study compared the University of Georgia's original SPectral Ocean Color (SPOC) 3U cubesat frame to one redesigned out of PEEK that underwent structural, modal, and thermal finite-element simulations to validate topology optimization algorithms on PEEK satellite frames. The experimental results of the modal and structural TO of the frame was able to achieve the mission demands set forth by the launch provider while removing 106.8g when compared to the Aluminum frame.

The thermal analysis confirmed that the 3D printing process does introduce complications with the further development of TO structures. The thermomechanical design suggested that the current thermal conductivity of 0.32 W/mK is too low to mitigate the effects of hot spots generated during normal operation. Compared with aluminum alloys, the thermal conductivity of PEEK polymers are orders of magnitude smaller than that of metal components. This suggests potential deformation over the length of the mission as concentrated areas touching the payload could result in temperatures nearing the glass temperature of the material.

The results of this study provide a novel approach to FDM PEEK space applications which can be applied outside the scope of just satellite frames. Although there were thermomechanical challenges associated with integrating a TO frame for a 3U payload, smaller components would be more manageable to produce for future missions.

Acknowledgments

The authors would like to thank the University of Georgia Small Satellite Research Laboratory for allowing us the opportunity to not only enter but now contribute to the small satellite field. The knowledge and expertise of everyone in the lab is tremendous and we would not be here without them;

Bowen O'Steen, who was instrumental in helping us get as far as we did, even if we weren't able to implement everything he suggested. We sincerely thank you for your help;

And finally, The University of Georgia Center for Undergraduate Research has provided us the means of travelling to the 36th Annual Small Satellite Conference. This contribution has allowed all of us to begin realizing our ambitions as researchers so thank you.

References

1. Rinaldi, M., Cecchini, F., Pigliaru, L., Ghidini, T., Lumaca, F., & Nanni, F. (2020). Additive manufacturing of polyether ether ketone (PEEK) for space applications: A nanosat polymeric structure. *Polymers*, *13*(1), 11. https://doi.org/10.3390/polym13010011

2. Zanjanijam, A. R., Major, I., Lyons, J. G., Lafont, U., & Devine, D. M. (2020). Fused filament fabrication of Peek: A review of process-structure-property relationships. *Polymers*, *12*(8), 1665. https://doi.org/10.3390/polym12081665
3. Arif, M. F., Kumar, S., Varadarajan, K. M., & Cantwell, W. J. (2018). Performance of biocompatible peek processed by fused deposition additive manufacturing. *Materials & Design*, *146*, 249–259. https://doi.org/10.1016/j.matdes.2018.03.015
4. Pu, J., McIlroy, C., Jones, A., & Ashcroft, I. (2021). Understanding mechanical properties in fused filament fabrication of polyether ether ketone. *Additive Manufacturing*, *37*, 101673. https://doi.org/10.1016/j.addma.2020.101673
5. Wu, W., Geng, P., Li, G., Zhao, D., Zhang, H., & Zhao, J. (2015). Influence of layer thickness and raster angle on the mechanical properties of 3D-printed peek and a comparative mechanical study between Peek and ABS. *Materials*, *8*(9), 5834–5846. https://doi.org/10.3390/ma8095271
6. Yang, C., Tian, X., Li, D., Cao, Y., Zhao, F., & Shi, C. (2017). Influence of thermal processing conditions in 3D printing on the crystallinity and mechanical properties of Peek

Material. *Journal of Materials Processing Technology*, *248*, 1–7. https://doi.org/10.1016/j.jmatprotec.2017.04.027
7. Wang, P., Zou, B., Xiao, H., Ding, S., & Huang, C. (2019). Effects of printing parameters of fused deposition modeling on mechanical properties, surface quality, and microstructure of Peek. *Journal of Materials Processing Technology*, *271*, 62–74. https://doi.org/10.1016/j.jmatprotec.2019.03.016
8. Basgul, C., Yu, T., MacDonald, D. W., Siskey, R., Marcolongo, M., & Kurtz, S. M. (2018). Structure–property relationships for 3D-printed peek intervertebral lumbar cages produced using fused filament fabrication. *Journal of Materials Research*, *33*(14), 2040–2051. https://doi.org/10.1557/jmr.2018.178
9. Singh, S., Prakash, C., & Ramakrishna, S. (2019). 3D printing of polyether-ether-ketone for biomedical applications. *European Polymer Journal*, *114*, 234–248. https://doi.org/10.1016/j.eurpolymj.2019.02.035
10. Space product assurance. thermal vacuum outgassing test for the screening of Space Materials. (n.d.). https://doi.org/10.3403/02527704u
11. Hopkins, J. B., Song, Y., Lee, H., Fang, N. X., & Spadaccini, C. M. (2016). Polytope sector-based synthesis and analysis of microstructural architectures with tunable thermal conductivity and expansion. *Journal of Mechanical Design*, *138*(5). https://doi.org/10.1115/1.4032809
12. Rinaldi, M., Ferrara, M., Pigliaru, L., Allegranza, C., & Nanni, F. (2021). Additive manufacturing of polyether ether ketone-based composites for space application: A mini-review. *CEAS Space Journal*. https://doi.org/10.1007/s12567-021-00401-4
13. Wu, W. Z., Geng, P., Zhao, J., Zhang, Y., Rosen, D. W., & Zhang, H. B. (2014). Manufacture and thermal deformation analysis of semicrystalline polymer polyether ether ketone by 3D printing. *Materials Research Innovations*, *18*(sup5). https://doi.org/10.1179/1432891714z.0000000000898
14. *Victrex Peek 450p*. (n.d.). Retrieved June 3, 2022, from https://www.victrex.com/-/media/downloads/datasheets/victrex_tds_450p.pdf?rev=7b144561ee104c9c8af52e06c64621d7
15. *Selection case study: Thermo-mechanical applications - ansys*. (n.d.). Retrieved June 3, 2022, from https://www.ansys.com/content/dam/amp/2021/august/webpage-requests/education-resources-dam-upload-batch-1/sel-case-study-thermo-mechanical-CASCSTEN21.pdf
16. Mourhatch, R. (2017, June 20). *NASA Jet Propulsion Laboratory (JPL) - robotic space exploration*. NASA. Retrieved July 14, 2022, from https://www.jpl.nasa.gov/
17. *Antares User's Guide - Northrop Grumman*. (2020, September). Retrieved July 15, 2022, from https://www.northropgrumman.com/wp-content/uploads/Antares-User-Guide-1.pdf
18. Basgul, C., Yu, T., MacDonald, D. W., Siskey, R., Marcolongo, M., & Kurtz, S. M. (2019). Does annealing improve the interlayer adhesion and structural integrity of FFF 3D printed Peek Lumbar Spinal Cages? *Journal of the Mechanical Behavior of Biomedical Materials*, *102*, 103455. https://doi.org/10.1016/j.jmbbm.2019.103455
19. Tseng, J.-W., Liua, C.-Y., Yen, Y.-K., Belkner, J., Liu, B. H., Sun, T.-J., & Wang, A.-B. (2017). Additive manufacturing - material extrusion-based additive manufacturing of plastic materials. https://doi.org/10.3403/bsenisoastm52903
20. Jared. "What Is the PSD? - Vibration Testing & Analysis - Power Spectral Density." *VRU*, 31 May 2022, https://vru.vibrationresearch.com/lesson/what-is-the-psd/.
21. He, E. M., Yin, G. L., & Hu, Y. Q. (2013). Random Vibration Analysis and Structural Modification of Satellite-Borne Equipment. In Applied Mechanics and Materials (Vol. 455, pp. 310–313). Trans Tech Publications, Ltd. https://doi.org/10.4028/www.scientific.net/amm.455.310
22. Alawadhi, E.M. (2010). Finite Element Simulations Using ANSYS (1st ed.). CRC Press. https://doi.org/10.1201/9781439801611
23. Barsoum, G., Ibrahim, H., & Fawzy, M. (2019, July 1). IOPscience. Journal of Physics: Conference Series. Retrieved August 6, 2022, https://iopscience.iop.org/article/10.1088/1742-6596/1264/1/012019/meta
24. Shukla, D., Negi, Y. S., Uppadhyaya, J. S., & Kumar, V. (2011, December 20). Synthesis and modification of poly(ether ether ketone) and their properties: A Review. Taylor & Francis. Retrieved August 6, 2022, https://www.tandfonline.com/doi/full/10.1080/15583724.2012.668151
25. Jones, D. P., Leach, D. C., & Moore, D. R. (2003, April 22). Mechanical properties of

poly(ether-ether-ketone) for engineering applications. ScienceDirect. Retrieved August 6, 2022, https://www.sciencedirect.com/science/article/pii/0032386185903167